


RESEARCH

Open Access



# Functionalized chitosan-G-poly caprolactone vaccine delivery system fabricated to display antigen–antibody immune complexes of *Mycobacterium tuberculosis* elicits immune response in *Ex-vivo* model

Sam Ebenezer Rajadas<sup>1,4</sup> , Vignesh Sounderrajan<sup>1,4</sup>, Rajendran Amarnath Prabhakaran<sup>2</sup>, Ragini Agrawal<sup>1</sup>, Lavanya Jeyadoss<sup>3</sup>, Mariappan Rajan<sup>2</sup>, Krupakar Parthasarathy<sup>4</sup> and Shakila Harshavardhan<sup>1\*</sup>

## Abstract

**Background** Vaccine development against tuberculosis remains a global health imperative, necessitating robust immunogenicity and safety profiles. Nanoparticle-based delivery systems offer promising avenues to enhance vaccine efficacy while ensuring tolerability. This study explores the utilization of chitosan micelles as a delivery platform for immune complex vaccination against tuberculosis. Leveraging two key antigens of *Mycobacterium tuberculosis*, namely HspX and Mpt51, known for their relevance in latent tuberculosis and its co-infection with the human immunodeficiency virus, immune complexes were synthesized *in vitro* using antibodies raised against these antigens. The immune complexes were then conjugated onto chitosan micelles, characterized for their physicochemical properties, and evaluated for their biocompatibility and immunogenicity.

**Results** Chitosan nanoparticles conjugated with either antigen or its immune complexes were synthesized as micelles and physicochemical characterizations confirm the formation of micelles without altering the polymer composition. These immune complex-conjugated chitosan micelles were found to be safe, exhibiting no significant hemolytic and cytotoxic activity even at a higher concentration of 400 µg/ml. Peripheral blood mononuclear cells upon stimulation with immune complex-conjugated chitosan micelles showed enhanced cellular uptake and one to two-fold increased expression of key immune markers—interferon gamma and CD-86.

**Conclusions** These findings underscore the potential of chitosan nanoparticles as a versatile delivery platform for immune complex vaccination against tuberculosis. While limitations exist, such as including only two markers of immune modulation, this study lays a foundation for future investigations into immune complex vaccine potential in animal models. In conclusion, chitosan micelles carrying immune complexes of HspX and Mpt51 tuberculosis antigens exhibit promising immunogenicity, highlighting their potential as a platform for multi-antigenic vaccine components warranting further *in vivo* studies.

**Keywords** Chitosan, Nanovaccine delivery, Tuberculosis, Immune complexes, Micelles

\*Correspondence:

Shakila Harshavardhan  
mohanshakila@yahoo.com

Full list of author information is available at the end of the article



© The Author(s) 2024. **Open Access** This article is licensed under a Creative Commons Attribution 4.0 International License, which permits use, sharing, adaptation, distribution and reproduction in any medium or format, as long as you give appropriate credit to the original author(s) and the source, provide a link to the Creative Commons licence, and indicate if changes were made. The images or other third party material in this article are included in the article's Creative Commons licence, unless indicated otherwise in a credit line to the material. If material is not included in the article's Creative Commons licence and your intended use is not permitted by statutory regulation or exceeds the permitted use, you will need to obtain permission directly from the copyright holder. To view a copy of this licence, visit <http://creativecommons.org/licenses/by/4.0/>.

## 1 Background

The cornerstone of vaccine research lies in achieving robust immunogenicity while ensuring safety and tolerability. Early vaccine formulations often elicited durable immune responses but were associated with poor tolerability. To address this challenge, researchers have focused on developing vaccine candidates incorporated into suitable delivery systems that mimic key immunogenic features such as the size, shape, and surface molecule organization of infectious agents. These systems not only enhance antigen presentation to immune cells but also improve overall immune responses [1]. One critical strategy to enhance vaccine potency is the inclusion of adjuvants, particularly molecular adjuvants, which boost vaccine efficacy without causing adverse effects. Examples of such adjuvants include granulocyte-monocyte colony-stimulating factor (GM-CSF), pathogen-associated molecular patterns (PAMPs), and the Fc portion of immunoglobulin G (IgG-Fc) [2–4]. Moreover, vaccine delivery methods play a crucial role in determining efficacy [5].

Recent research has focused on leveraging nanoparticles (NPs) as efficient vaccine delivery vehicles. NPs can encapsulate vaccine antigens or display them on their surface, protecting against antigen degradation and promoting sustained immune responses [6]. By mimicking the presentation pattern of antigen-presenting cells (APCs), NPs facilitate robust immune responses. Various nanocarrier systems such as solid gold NPs, chitosan NPs (CNPs), liposomes, and microspheres enable diverse delivery routes like topical application, inhalation, intracellular delivery, and multiplexing [5–7]. CNPs stand out for their adjuvant properties, enhancing cytokine responses and T cell-mediated immunity [8]. Chitosan, an FDA-approved non-toxic and biocompatible substance, makes CNPs suitable for clinical use [9]. Additionally, CNPs' muco-adhesive properties make them promising for intranasal vaccine delivery, eliminating the need for injections [10, 11].

Previous studies from our group highlighted the immunomodulatory potential of immune complexes (ICs) during tuberculosis (TB) infection that conferred protection to *Mycobacterium tuberculosis* (Mtb) infected guinea pigs [12]. IC administration showed protective effects in guinea pig models, reducing pathogen load, and influencing macrophage polarization and granuloma formation. Similar findings were observed in *ex-vivo* models using the *in vitro* 3D granuloma model and ICs conjugated with Mtb antigens HspX and Mpt51 (Unpublished data). Notably, the HspX antigen, highly expressed during TB latency, is considered a vaccine candidate against Mtb infection, and Mpt51 is an immunodominant antigen with diagnostic importance [13–16]. Our findings

suggest that ICs can modulate host immune responses and may serve as potential vaccine candidates, leveraging the adjuvant properties of IgG-Fc portions. In this study, we aimed to develop a chitosan micellar nanoparticle-based delivery system for efficient IC vaccine delivery. We characterized its physicochemical and functional properties through rigorous *in vitro* and *ex-vivo* analysis, laying the groundwork for potential future vaccine development strategies.

## 2 Methods

### 2.1 In vitro synthesis of ICs

Mtb antigens (HspX and Mpt51) used in the IC preparation were previously expressed and purified in-house using recombinant *E.coli* BL21 that was heterologously transformed with *hspX* and *mpt51* genes. The polyclonal antibodies against these antigens were also prepared in-house by immunizing the rabbits with corresponding antigens (Additional file 1: Fig. 1). The IgG antibodies from the serum of immunized rabbits were separated using Ni–NTA column chromatography as instructed by the manufacturer (HiMedia, India). The functional characterization of the purified antibodies was done by performing an enzyme-linked immune-sorbent assay (ELISA) and serum bactericidal assay (Additional file 2, 3, 4: Figs. 2 to 4).

ICs composed of HspX and Mpt51 antigens and their respective polyclonal antibodies were synthesized *in vitro* by adapting the methods as described elsewhere. In brief, equal concentrations and volumes of antigen and purified antibody were mixed (HspX antigen with anti-HspX antibody and Mpt51 antigen with anti-Mpt51 antibody) and incubated at 37 °C for 2 hours (h). To this, equal volume of 7% polyethylene glycol (PEG) 4000 was added to make a final concentration of 3.5% and allowed to precipitate at 4 °C overnight. Post-incubation, it was centrifuged at 13000 rpm at 4 °C for 10 min. The pellet was washed with 3.5% PEG twice and suspended in 1X phosphate-buffered saline (PBS).

### 2.2 Estimation of Zeta potential of antigens and ICs

Efficient conjugation of ICs and antigens on the CNPs depends on their total charges. The surface charge of chitosan is positive and hence readily binds with the negatively charged compounds [17]. The surface charge of the HspX, Mpt51 antigens, antibodies, and ICs was identified using dynamic light scattering (DLS) Delsa Nano C Particle analyzer (Beckman Coulter, USA), before carrying out the nanoparticle synthesis.

### 2.3 Synthesis of chitosan-G-poly caprolactone

The chitosan-G-poly caprolactone (Cs-g-PCL) delivery system was synthesized in the laboratory by following

the in-house procedure that is employed by ring-opening polymerization [18]. In brief, chitosan (6 mmol glucosamine units) was vacuum-dried and mixed with methanesulfonic acid solvent, and  $\epsilon$ -CL monomer (52 mmol) in a glass ampoule under  $N_2$  at 45 °C. After dissolution, the mixture was irradiated under reduced pressure, cooled, and dropped into a solution of 0.2 M  $KH_2PO_4$ , 10 M NaOH, and ice (50 g). The filtrate was washed and dialyzed against deionized water and then lyophilized to obtain the product.

#### 2.4 Synthesis of antigen and IC-conjugated CS-g-PCL micelles

CS-g-PCL polymer 100 mg was dissolved in 2 ml dimethyl sulfoxide (DMSO) and autoclaved. Antigens and ICs (HspX, anti-HspX, Mpt51, anti-Mpt51) were added dropwise to the solution along with 1 ml of 1% acetic acid and then stirred continuously. The mixture underwent three cycles of ultrasonication (30 s each) with intervals in an ice bath. Subsequently, it was dialyzed against 200 ml ultrapure water for 24 h, with water changes every 4 h, to remove organic solvents. The purified antigen and IC-conjugated CNPs were stored under refrigeration until further use.

#### 2.5 Physiochemical characterization of IC-conjugated Chitosan-based delivery system

The IC-conjugated Cs-g-PCL delivery system was subjected to physiochemical characterization using various techniques as described previously [19]. Fourier transform infrared (FTIR) spectra were obtained with a Thermo Nicolet 6700 spectrophotometer, USA. Wide-angle X-ray diffraction (XRD) analysis was conducted using a Philips 1710 X-ray diffractometer (Netherlands) with the copper target. Scanning electron microscopy (SEM, VEGA3 TESCAN, Czech Republic) was performed after the gold-palladium coating of samples using a sputter coater (VEGA3SB, Czech Republic). Transmission electron microscopy (TEM) was carried out using a JEOL JEM 1400 (Japan). The shape and size of nanoparticles were determined on a carbon-coated copper grid.

#### 2.6 Ex-vivo immunological characterization of IC-conjugated chitosan delivery system

The potential of the IC-conjugated chitosan delivery system to induce immune response was tested *ex-vivo* on peripheral blood mononuclear cells (PBMCs) (HiMedia, India) and U937 cells (NCCS, Pune).

##### 2.6.1 Stimulation of PBMCs with, antigen and IC-conjugated chitosan delivery system

Post-24 h of PBMC revival, cells were treated with chitosan micelles conjugated with antigens and ICs (HspX and Mpt51, 20  $\mu$ g/ml each). Phorbol 12-myristate 13-acetate (PMA) (5 ng/ml) served as a positive control for PBMC induction. Incubation occurred at 37 °C in a 5%  $CO_2$  atmosphere, with morphological changes observed.

Similarly, U937 cells and PBMCs were treated with rhodamine-tagged CNPs to assess internalization capability. After 60 min of stimulation, cells were observed under a fluorescent inverted phase-contrast microscope.

After 72 h of stimulation, PBMCs were harvested for RNA isolation using a HiPur-A kit (HiMedia, India). Isolated total RNA purity and integrity were checked using nanodrop spectrophotometer analysis and RNA gel electrophoresis. cDNA was synthesized from RNA using a Protoscript II reverse transcriptase cDNA synthesis kit (New England Biologicals, USA). The RNA template concentration was maintained constant (1  $\mu$ g). The expression of interferon- $\gamma$  (IFN- $\gamma$ ) and CD-86, a marker for monocyte activation into macrophages, was assessed using cDNA as a template.

Real-time PCR was performed using the ABI-7000 real-time PCR machine (Applied Biosystems, USA) (DST PURSE Facility at School of Biotechnology, Madurai Kamaraj University). The reaction mixture comprised Syber Green master mix (Roche, Switzerland) and specific primers (Table 1). Reaction conditions included denaturation for 60 s, annealing for 45 s, and extension for 30 s, adjusted based on the primer sequence and PCR product length. The dissociation constant was monitored to ensure reaction specificity. All the experiments were carried out in triplicates with untreated PBMCs as control, and the statistically significant difference was determined through Student's *t*-test between IC and non-IC groups using GraphPad Prism software version for

**Table 1** List of PCR primers used to study the induction of immune response by IC-loaded Cs-g-PCL in Monocytes

Cytokines	Forward Primer (5'–3')	Reverse Primer (5'–3')
$\beta$ -Actin	TCACCCACACTGTGCCCATCTACG	CAGCGGAACCGCTCATTGCCAATG
IFN $\gamma$	AGCTCTGCATCGTTTTGGGT	CGCTTCCCTGTTTTAGCTGC
CD-86	CCATCAGCTTGCTGTTTCATTCC	GCTGTAATCCAAGGAATGTGGTC

Windows (GraphPad Software Inc., La Jolla, CA, USA). *P* value less than 0.05 was considered significant.

### 2.7 Cell proliferation and cytotoxicity assay

The impact of CNPs on cell viability and growth in PBMCs was assessed using the EZcount™ MTT cell assay kit (Himedia, India) following the methods as described previously [20]. In brief,  $1 \times 10^4$  PBMCs were seeded per well in 96-well plates and incubated overnight under standard growth conditions. They were then treated with synthesized CNPs at concentrations of 50, 100, 200, and 400  $\mu\text{g/ml}$ . After 24 h of incubation, cells were treated with 10% MTT solution and incubated at 37 °C until blue crystals formed (3–4 h). Subsequently, the cells were disrupted and blue crystals were dissolved by adding an equal volume of solubilization buffer. Spectrophotometric readings were taken at 570 nm and 630 nm wavelengths using the Multiskan EX instrument (Thermo Scientific, USA). Cell viability percentage was calculated using the equation given below after subtracting the absorbance value at 630 nm from that at 570 nm. These procedures were performed in triplicates.

$$\text{Cell viability(\%)} = \frac{(\text{Absorbance of test} - \text{Absorbance of blank})}{(\text{absorbance of control} - \text{Absorbance of blank})} \times 100$$

### 2.8 Hemolytic activity test

To assess the biocompatibility of the synthesized CNPs, it was further tested on the red blood cells (RBCs) following the protocol mentioned elsewhere [20–22]. In summary, RBCs were isolated from whole blood through centrifugation and washed twice with PBS to eliminate serum complement proteins. They were then diluted 1:10 with PBS. Diluted RBCs (200  $\mu\text{l}$ ) were mixed with 1000  $\mu\text{l}$  of the test solutions to achieve final concentrations of 50, 100, 200, and 400  $\mu\text{g/ml}$ . Distilled water and PBS were used as positive and negative controls, respectively. Cell suspensions were gently mixed, incubated at 37 °C for 2 h, and then centrifuged at 4000g for 10 min at 4 °C. The supernatant was collected, and absorbance at 541 nm was measured using the Multiskan EX instrument (Thermo Scientific, USA). The analysis was conducted in triplicates. The percentage of hemolysis was calculated using the formula,

$$\text{Hemolytic activity(\%)} = \frac{(\text{Absorbance of test} - \text{Absorbance of negative control})}{(\text{absorbance of Positive control} - \text{Absorbance of negative control})} \times 100$$

## 3 Results

### 3.1 Determination of Zeta potential

Zeta potential is determined to find the surface charge of the particles based on the principle of electrophoretic

**Table 2** Surface Charges for HspX antigen, anti-HspX antibody, Mpt51 antigen, and anti-Mpt51 antibodies

Proteins	mV
Anti-HspX	– 17.35
HspX	– 15.60
Anti-Mpt51	– 16.20
Mpt51	– 13.46

light scattering as the binding of proteins to the nanoparticles is based on the charge. HspX antigen, Mpt51 antigen, and respective antibodies possessed a negative charge on their surfaces (Table 2 and Fig. 1).

### 3.2 Physicochemical characterization of IC-conjugated chitosan-based delivery system

The FTIR spectrum of the synthesized chitosan micelles (Fig. 2) reveals specific absorption peaks at 2920  $\text{cm}^{-1}$  and 1251  $\text{cm}^{-1}$ . These peaks are attributed to the -CH<sub>3</sub> groups and C–O–C stretching vibrations, respectively, which are characteristic of the SA-g-AA (sodium algi-

nate-grafted-acrylic acid) component within the micelles. The incorporation ICs did not induce any significant changes in the FTIR spectrum of the CNPs, indicating that the primary chemical structure of the CNPs remains intact after complexation with the antigens and antibodies. XRD analysis provided further insight into the structural modifications of the chitosan micelles upon the incorporation of ICs. As shown in Fig. 3, a new broad peak emerged in the XRD pattern, signifying a transition in the physical state of the material from an amorphous to a semi-crystalline form. This transformation suggests that the micelles have undergone a degree of ordering, potentially due to interactions between the chitosan polymer matrix and the incorporated ICs. The morphological characteristics of the micelles were examined using SEM and TEM. SEM images (Fig. 4) revealed the successful formation of micelles following the incorporation of antigens, and ICs specific to HspX and Mpt51. The size

distribution of these micelles ranged from 100 to 200 nm, demonstrating a uniform and controlled synthesis process. The TEM images (Fig. 5) corroborated the SEM findings, showcasing well-defined micellar structures.

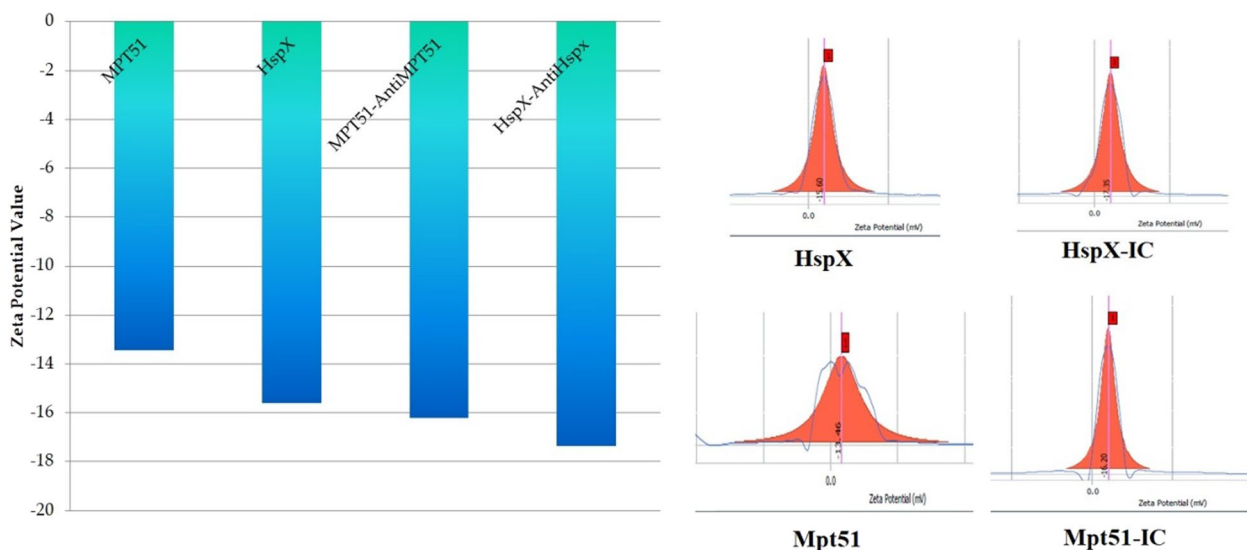


**Fig. 1** The zeta-potential value of HspX and Mpt51 antigens and their respective ICs. The values expressed as mV are in negative delineation, favoring effective conjugation with the CNPs

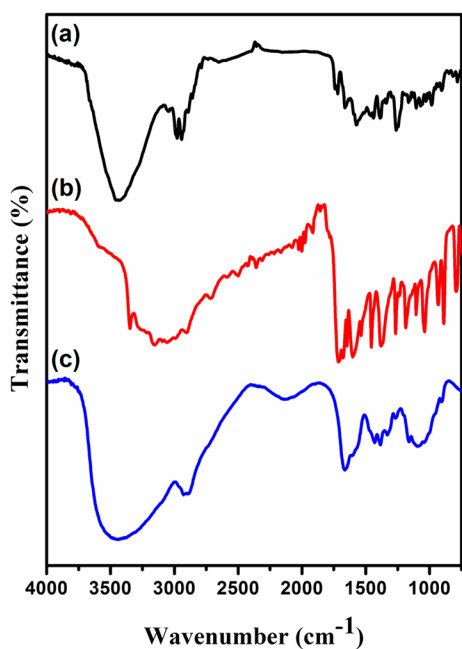


**Fig. 2** FTIR spectrum of Chitosan Micelles loaded with the antigen and ICs of HspX and Mpt51. **a** Chitosan micelles conjugated with HspX, Mpt51, and its respective ICs; **b** Empty Chitosan micelles; **c** Chitosan polymer before grafting

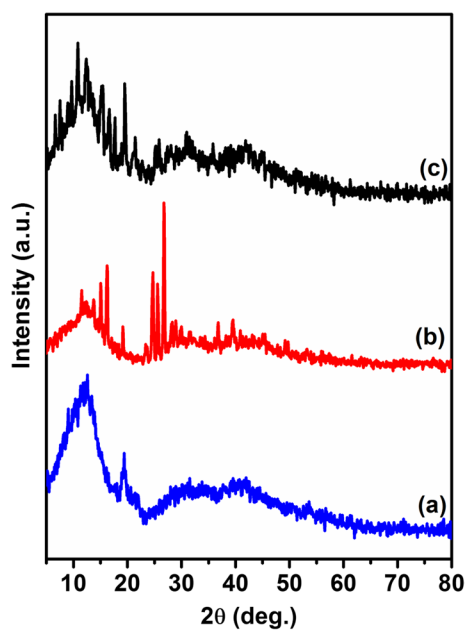


**Fig. 3** XRD pattern of Chitosan Micelles. **a** Chitosan polymer before grafting; **b** empty Chitosan micelles; **c** Chitosan micelles conjugated with HspX, Mpt51, and its respective ICs

Interestingly, the TEM analysis also revealed the presence of smaller micellar formations at the periphery of the larger micelles. This phenomenon suggests a hierarchical organization within the micellar assembly, possibly indicating secondary self-assembly processes or interactions between different components within the micelles.

### 3.3 Biocompatible nature of the CNPs

The biocompatible nature of the IC-conjugated CNPs was tested on the PBMCs and RBCs. It was found to be completely safe even up to 400 µg/ml (Fig. 6). There was a significantly lesser hemolytic activity (2%) only at the higher concentration of 400 µg/ml of the CNPs (Fig. 7).



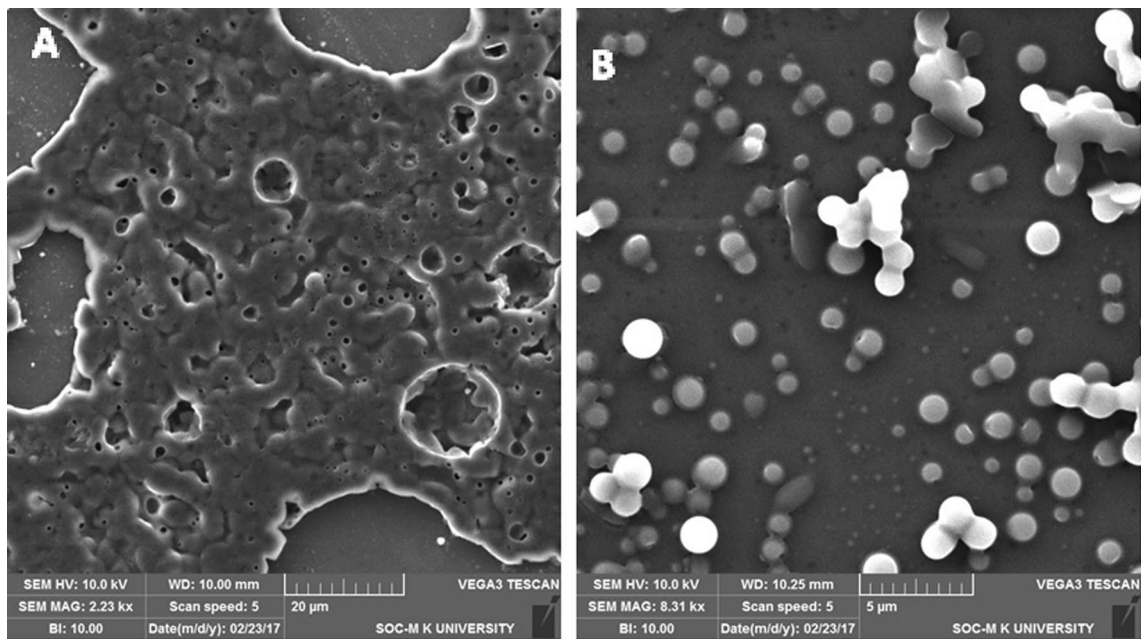


**Fig. 4** SEM micrographs showing the Chitosan-based polymer before (a) and after (b) micelle formation. The formation of micelles can be observed (Magnification: 14,000 X)

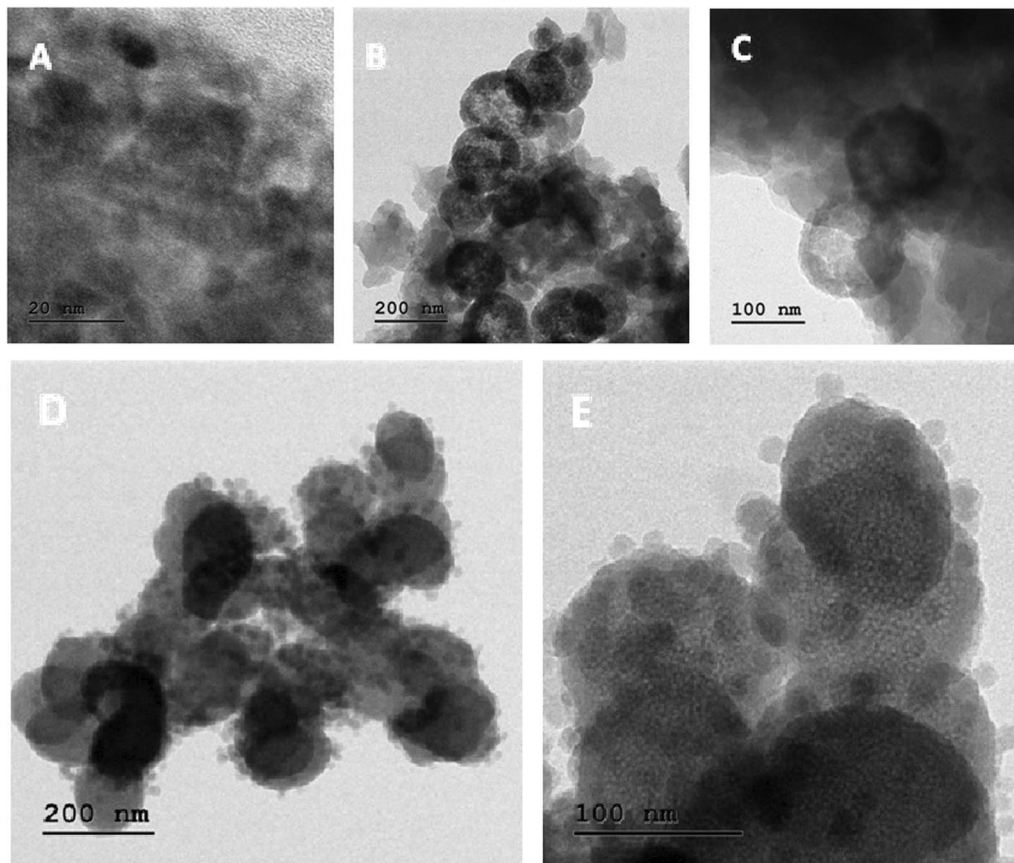


**Fig. 5** TEM micrographs showing the Chitosan-based polymer before (a) and after (b, c) micelle formation. Conjugation of the ICs could be observed on the surface of the micellar structure (d, e) (Magnification: 25,000 X)

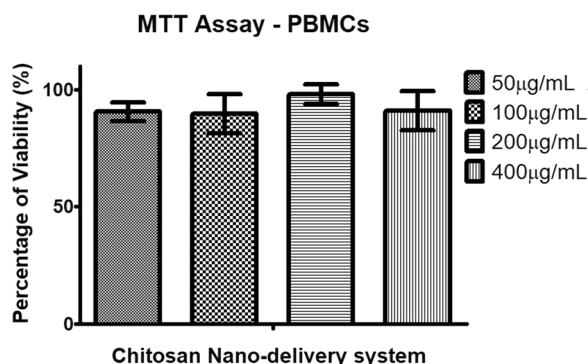


**Fig. 6** Percentage of cell viability of the PBMCs treated with CNPs. The values are compared with the control cells, which were given mock treatment with PBS

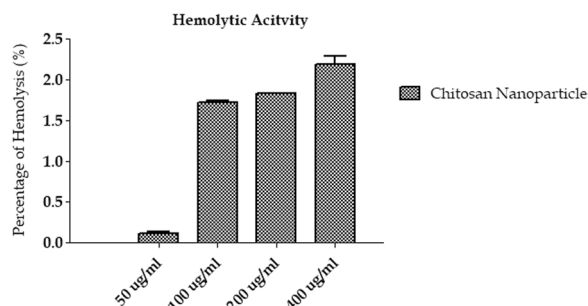


**Fig. 7** Percentage of hemolysis of the RBCs treated with CNPs. The values are compared with the control cells, which were treated with PBS (negative control) and water (Positive control)

**3.4 Functional characterization of CNP delivery system**

After 60 min of stimulation, the CNPs were also internalized by the U937 cells and PBMCs (Fig. 8) and the cells showed morphological evidence of differentiation of monocytes into macrophages.

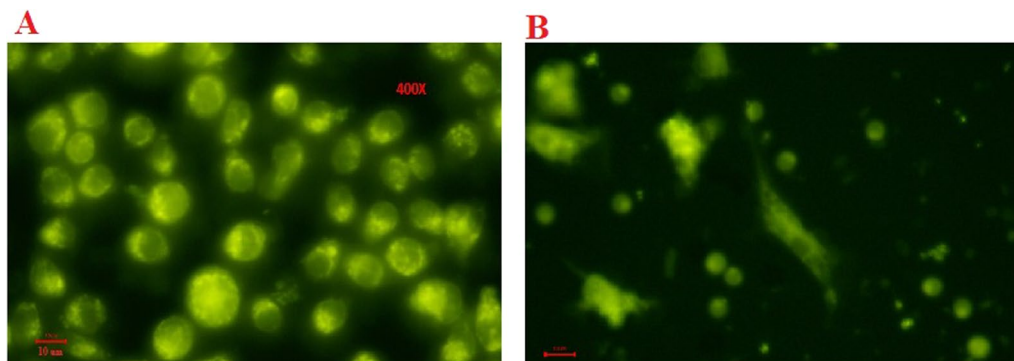


**Fig. 8** Internalization of CNPs by U937 cells (a) and PBMCs (b) Changes in the morphology like the formation of pseudopods and differentiation of the PBMCs could be observed due to the activation of cells after 1 h (b). Magnification at 400X (scale 10 µm)

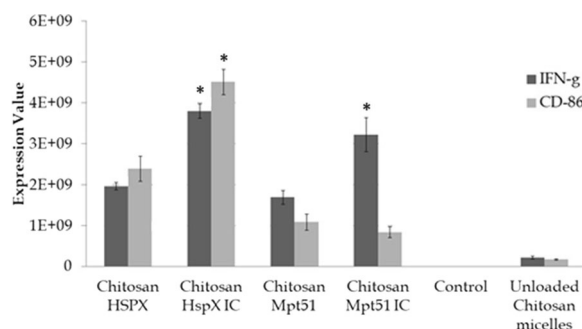


**Fig. 9** Differential expressions of IFN-γ and CD-86 by the PBMCs induced with CNPs conjugated with the HspX & Mpt51 antigens and their respective ICs. \*  $P < 0.05$  compared to PBMCs induced with CNPs conjugated with respective antigens alone

IC-conjugated CNPs were found to induce the expression of IFN-γ and CD-86 (Fig. 9). This indicates the activation and differentiation of the monocytes supporting the above observations related to changes in the morphology of the cells. Further, the CD-86 marker represents the activation of T cells by the activated monocytes, favoring cell-mediated immunity's involvement.

**4 Discussion**

Despite extensive scientific efforts spanning centuries, TB remains a formidable global health challenge, persisting with an incidence rate of 182 per 0.1 million individuals and claiming the lives of 24 per 0.1 million people worldwide. The association between TB and HIV is well known. However, more than HIV, malnutrition is accounted as a major predisposing factor that triggers TB disease progression in the patients. Seven percent of drug-sensitive and 26% of drug-resistant TB patients either fail or poorly respond to anti-TB treatment due to various factors [23]. This emphasizes the role of host

factors in combating this pathogen. The BCG vaccine, currently the only approved vaccine for TB, lacks effectiveness in providing adequate protection for the adult population due to its inability to induce a strong memory response, despite triggering Th1 immune responses [24]. Consequently, there is an urgent demand for a highly efficient TB vaccine capable of safeguarding adults, both adult and pediatric populations. To address this need, various strategies such as subunit vaccines and whole antigen vaccines combined with adjuvants are being pursued [25].

This study aimed to advance our understanding based on our previous findings highlighting the importance of ICs in eliciting a protective immune response compared to free antigens. We selected two antigens from *Mtb*, specifically HspX and Mpt51, known for their relevance in latent TB and HIV-TB co-infection scenarios. To prepare ICs, we utilized antibodies raised in rabbits immunized separately with HspX and Mpt51 (Additional files 1, 2, 3, 4: Figs. 1 to 4). These ICs were then made to attach onto chitosan micelles, characterized for their physicochemical properties, to emulate natural antigen presentation within the host (Figs. 4 and 5). Subsequently, we evaluated the biocompatibility of these IC-conjugated chitosan micelles on PBMCs and RBCs. Our results indicate that even at a concentration of 400  $\mu\text{g/mL}$ , these micelles are safe and do not induce significant hemolysis (Figs. 6 and 7). Notably, prior studies have also affirmed similar findings, reinforcing the safety of these micelles within the physiological system [26].

IC-conjugated CNPS was found to enhance the cellular uptake and activation of PBMCs within 60 min post-stimulation, leading to increased expression of IFN- $\gamma$  and CD-86, indicating type-I interferon activation, macrophage, T cell, and B cell activation (Figs. 8 and 9). Expression of IFN- $\gamma$  and CD-86 was comparatively lower when the cells were induced with antigen alone containing chitosan micelles. This shows the significance of the IgG-Fc portion in the ICs in inducing an immune response, especially during TB infection. IFN- $\gamma$  plays a vital role by activating the macrophages and subsequently inducing the Th1 proliferation to promote inflammation and curtail TB progression. The same is found to increase during latent TB also [27]. On the other hand, CD-86 also indicates the activation of macrophages besides the B cells [28].

Previous studies have demonstrated the adjuvant properties of CNPs. For instance, a Chitosan nanoparticle carrying the H1N1 influenza viral antigen enhanced antibody titers up to threefold compared to conventional adjuvants like alum [29]. Moreover, a mice model challenged with *Schistosoma mansoni* infection following immunization with a DNA vaccine delivered through

Chitosan exhibited 47% protection, even when administered orally [30]. CNPs are also suitable for intranasal administration, mimicking TB's pulmonary route of infection. Studies in chickens administering a formulation carrying antigens of Newcastle disease (ND) and infectious bronchitis (IB) intranasally displayed higher IgA and IgG titers. Additionally, CNPs have been shown to enhance cellular uptake and activation of immune cells such as THP-1 monocytes and dendritic cells [31]. Hence, it could be claimed that when the antigens HspX and Mpt51 are presented as ICs it could induce higher cell proliferation, and activation of macrophages, T cells, and B cells that are very much required for the efficacy of a vaccine. These chitosan-based micelle-shaped delivery systems are incorporated with antigens and their ICs. Physicochemical characterizations confirm the formation of micelles without altering the polymer composition (Figs. 2 and 3). While prior research has explored the use of chitosan particles as delivery systems for immunization and vaccination against various toxins, infectious agents (bacterial and viral), proteins, and DNA, this study marks the first attempt to utilize these CNPs for IC vaccination purposes.

In summary, this study underscores the promising role of CNPs as a versatile delivery platform for IC vaccination against TB, offering potential improvement over existing vaccine strategies. The inclusion of only two markers of immune modulation is the major limitation that could be rectified in the next phase of the study to evaluate IC's vaccine potential in the non-infected and infected animal models.

## 5 Conclusion

This study highlights the potential of chitosan micelles conjugated with ICs of HspX and Mpt51 antigens as an innovative and effective approach for TB vaccination. The IC-conjugated chitosan micelles exhibited promising physicochemical properties and maintained biocompatibility, significantly enhancing the activation of PBMCs. This led to elevated expressions of critical immune markers such as IFN- $\gamma$  and CD-86, underscoring the importance of the IgG-Fc portion in ICs for eliciting a robust immune response. This response is crucial for combating TB infection and could significantly improve the efficacy of TB vaccines, especially for adults who are inadequately protected by the current BCG vaccine. The IgG-Fc portion could be used as a common platform to include additional immunodominant TB antigens in further studies. Although preliminary, this study lays a strong foundation for further development of chitosan-based micelle-shaped delivery systems in TB vaccination, offering a promising avenue for enhancing global TB control efforts.



## Abbreviations

APCs	Antigen-presenting cells
Cs-g-PCL	Chitosan-G-poly caprolactone
DMSO	Dimethyl sulfoxide
FTIR	Fourier transform infrared
GM-CSF	Granulocyte-monocyte colony-stimulating factor
ICs	Immune complex
IgG	Immunoglobulin G
Mtb	<i>Mycobacterium tuberculosis</i>
NPs	Nanoparticles
PAMPs	Pathogen-associated molecular patterns
PBMC	Peripheral blood mononuclear cells
PBS	Phosphate-buffered saline
PEG	Polyethylene glycol
PMA	Phorbol 12-myristate 13-acetate
RBC	Red blood cells
SEM	Scanning electron microscopy
TEM	Transmission electron microscopy
XRD	X-ray diffraction analysis

## Supplementary Information

The online version contains supplementary material available at <https://doi.org/10.1186/s43088-024-00520-x>.

Additional file 1.

Additional file 2.

Additional file 3.

Additional file 4.

## Acknowledgements

The authors thank the administrative staff of the School of Biotechnology, Madurai Kamaraj University (MKU) for helping manage the project funds. The authors also thank the technical staff of the SEM, TEM, and FTIR facilities of MKU.

## Author contributions

SER and SH conceptualized the study. VS performed heterologous expression of the Mtb antigens. SER and RA performed the production and purification of antibodies. SER, RAP, MR, and LJ performed experiments related to nanoparticle synthesis and characterization. SER, KP, and SH contributed manuscript writing. All authors read and approved the final manuscript.

## Funding

The authors thank DST PURSE for the SEM, TEM, and Fluorescence Microscopy facility and RUSA for the FTIR facility at Madurai Kamaraj University, India. SER and SH thank CSIR for financial support (No. 27(0289)/13/EMR-II Dated: 15.04.2013). VS thank UGC-BSR for fellowship (F-4-1/2006(BSR)/7-120/2007(BSR)).

## Availability of data and materials

The datasets used and/or analyzed during the current study are available from the corresponding author upon reasonable request.

## Declarations

### Ethics approval and consent to participate

The study was approved by the institutional ethics committee of Madurai Kamaraj University to handle Rabbits for raising antibodies against the two antigens—HspX and Mpt51.

### Consent for publication

Not applicable.

### Competing interests

The authors declare that they have no competing interests.

## Author details

<sup>1</sup>Department of Molecular Microbiology, School of Biotechnology, Madurai Kamaraj University, Madurai, Tamil Nadu 625021, India. <sup>2</sup>Department of Natural Chemistry, School of Chemistry, Madurai Kamaraj University, Madurai, Tamil Nadu 625021, India. <sup>3</sup>Department of Biotechnology, Periyar Maniammai Institute of Science and Technology, Vallam, Tamil Nadu, India. <sup>4</sup>Present Address: Centre for Drug Discovery and Development, Sathyabama Institute of Science and Technology, Chennai 600119, India.

Received: 11 April 2024 Accepted: 8 June 2024

Published online: 17 June 2024

## References

- Bachmann MF, Jennings GT (2010) Vaccine delivery: a matter of size, geometry, kinetics, and molecular patterns. *Nat Rev Immunol* 10:787–796. <https://doi.org/10.1038/nri2868>
- Mahla RS, Reddy MC, Prasad DVR, Kumar H (2013) Sweeten PAMPs: role of sugar complexed PAMPs in innate immunity and vaccine biology. *Front Immunol* 4:248
- Zhao W, Zhao G, Wang B (2018) Revisiting GM-CSF as an adjuvant for therapeutic vaccines. *Cell Mol Immunol* 15:187–189. <https://doi.org/10.1038/cmi.2017.105>
- Alleva DG, Delpero AR, Scully MM, Murikipudi S, Ragupathy R, Greaves EK et al (2021) Development of an IgG-Fc fusion COVID-19 subunit vaccine, AKS-452. *Vaccine* 39:6601–6613
- Mohan T, Verma P, Rao DN (2013) Novel adjuvants & delivery vehicles for vaccines development: a road ahead. *Indian J Med Res* 138:779–795
- Gregory AE, Titball R, Williamson D (2013) Vaccine delivery using nanoparticles. *Front Cell Infect Microbiol* 3:13
- Pati R, Shevtsov M, Sonawane A (2018) Nanoparticle vaccines against infectious diseases. *Front Immunol*. <https://doi.org/10.3389/fimmu.2018.02224>
- Feng G, Jiang Q, Xia M, Lu Y, Qiu W, Zhao D et al (2013) Enhanced immune response and protective effects of nano-chitosan-based DNA vaccine encoding T cell epitopes of Esat-6 and FL against *Mycobacterium tuberculosis* infection. *PLoS ONE* 8:e61135. <https://doi.org/10.1371/journal.pone.0061135>
- Malik A, Gupta M, Gupta V, Gogoi H, Bhatnagar R (2018) Novel application of trimethyl chitosan as an adjuvant in vaccine delivery. *Int J Nanomed* 13:7959–7970
- Pawar D, Jaganathan KS (2016) Mucoadhesive glycol chitosan nanoparticles for intranasal delivery of hepatitis B vaccine: enhancement of mucosal and systemic immune response. *Drug Deliv* 23:185–194. <https://doi.org/10.3109/10717544.2014.908427>
- Hajam IA, Senevirathne A, Hewawaduge C, Kim J, Lee JH (2020) Intranasally administered protein coated chitosan nanoparticles encapsulating influenza H9N2 HA2 and M2e mRNA molecules elicit protective immunity against avian influenza viruses in chickens. *Vet Res* 51:37. <https://doi.org/10.1186/s13567-020-00762-4>
- Ebenezer RS, Gupta UD, Gupta P, Shakila H (2017) Protective effect of antigen excess immune complex in Guinea pigs infected with *Mycobacterium tuberculosis*. *Indian J Med Res* 146:629–635
- Yousefi-Avarvand A, Tafaghodi M, Soleimanpour S, Khademi F (2018) HspX protein as a candidate vaccine against *Mycobacterium tuberculosis*: an overview. *Front Biol (Beijing)* 13:293–296. <https://doi.org/10.1007/s11515-018-1494-2>
- Achkar JM, Dong Y, Holzman RS, Belisle J, Kourbeti IS, Sherpa T et al (2006) *Mycobacterium tuberculosis* malate synthase- and MPT51-based serodiagnostic assay as an adjunct to rapid identification of pulmonary tuberculosis. *Clin Vaccine Immunol* 13:1291LP – 1293
- Bethunaickan R, Baulard AR, Loch C, Raja A (2007) Antibody response in pulmonary tuberculosis against recombinant 27kDa (MPT51, Rv3803c) protein of *Mycobacterium tuberculosis*. *Scand J Infect Dis* 39:867–874. <https://doi.org/10.1080/00365540701402954>
- de Sousa EM, da Costa AC, Trentini MM, de Araújo Filho JA, Kipnis A, Junqueira-Kipnis AP (2012) Immunogenicity of a fusion protein containing immunodominant epitopes of Ag85C, MPT51, and HspX from *Mycobacterium tuberculosis* in mice and active TB infection. *PLoS ONE* 7:e47781. <https://doi.org/10.1371/journal.pone.0047781>

17. Cheung RCF, Ng TB, Wong JH, Chan WY (2015) Chitosan: an update on potential biomedical and pharmaceutical applications. *Mar Drugs* 13:5156–5186
18. Yuan X, Amarnath Praphakar R, Munusamy MA, Alarfaj AA, Suresh Kumar S, Rajan M (2019) Mucoadhesive guar gum hydrogel inter-connected chitosan-g-polycaprolactone micelles for rifampicin delivery. *Carbohydr Polym* 206:1–10
19. Praphakar RA, Rajadas SE, Vignesh S, Shakila H, Rajan M (2019) Versatile pH-responsive chitosan-g-polycaprolactone/maleic anhydride—isoniazid polymeric micelle to improve the bioavailability of tuberculosis multidrugs. *Appl Biomater (ACS)* 565:1931–1943
20. Amarnath R, Sumathra M, Rajadas SE, Harshavardhan S, Rajan M (2019) Fabrication of bioactive rifampicin loaded  $\kappa$ -Car-MA-INH/nano hydroxyapatite composite for tuberculosis osteomyelitis infected tissue regeneration. *Int J Pharm* 565:543–556. <https://doi.org/10.1016/j.ijpharm.2019.05.035>
21. Alencar DB, Melo AA, Silva GC, Lima RL, Pires-Cavalcante KMS, Carneiro RF et al (2015) Antioxidant, hemolytic, antimicrobial, and cytotoxic activities of the tropical Atlantic marine zoanthid *Palythoa caribaeorum*. *An Acad Bras Cienc* 87:1113–1123
22. Slowing II, Wu C-W, Vivero-Escoto JL, Lin VS-Y (2009) Mesoporous silica nanoparticles for reducing hemolytic activity towards mammalian red blood cells. *Small* 5:57–62
23. WHO - Global Tuberculosis Programme. Global Tuberculosis Report—2023. Geneva; 2023 Nov
24. Andersen P, Woodworth JS (2014) Tuberculosis vaccines—rethinking the current paradigm. *Trends Immunol* 35:387–395
25. Tagliabue A, Boraschi D, Leite LCC, Kaufmann SHE (2022) 100 Years of BCG immunization: past, present, and future. *Vaccines (Basel)* 10:1743
26. Sonin D, Pochkaeva E, Zhuravskii S, Postnov V, Korolev D, Vasina L et al (2020) Biological Safety and biodistribution of chitosan nanoparticles. *Nanomaterials* 10:810
27. Shanmuganathan G, Orujyan D, Narinyan W, Poladian N, Dhama S, Parthasarathy A et al (2022) Role of interferons in *Mycobacterium tuberculosis* infection. *Clin Pract* 12:788–796
28. Axelsson S, Magnuson A, Lange A, Alshamari A, Hörnquist EH, Hultgren O (2020) A combination of the activation marker CD86 and the immune checkpoint marker B and T lymphocyte attenuator (BTLA) indicates a putative permissive activation state of B cell subtypes in healthy blood donors independent of age and sex. *BMC Immunol* 21:14
29. Dzung NA, Thi N, Hà N, Van DTH, Thi N, Phuong L et al (2011) Chitosan nanoparticles as a novel delivery system for H1N1 influenza vaccine: safe properties and immunogenicity in mice Chitosan nanoparticle as a novel delivery system for A/H1n1 influenza vaccine: safe property and immunogenicity in mice. *World Acad Sci Eng Technol* 5:915–922
30. Mohammadpour Dounighi N, Eskandari R, Zolfagharian H, Mohammad M (2012) Preparation and in vitro characterization of chitosan nanoparticles containing *Mesobuthus eupeus* scorpion venom as an antigen delivery system. *J Venom Anim Toxins Incl Trop Dis* 18:44–52
31. Hunsawong T, Sunintaboon P, Warit S, Thaisomboonsuk B, Jaram GR, Yoon I-K et al (2015) Immunogenic properties of a BCG adjuvanted chitosan nanoparticle-based dengue vaccine in human dendritic cells. *PLoS Negl Trop Dis* 9:1–18

## Publisher's Note

Springer Nature remains neutral with regard to jurisdictional claims in published maps and institutional affiliations.